POLYMERIC HYDROGELS WITH INCLUSION OF MAGNETIC NANOPARTICLES BY THE INVERSE MICROEMULSION METHOD

Ormaza Rosa[1,4*], Mayorga Yajaira[2], Mejía Nora[3], Aguilar Reyes Johanna[4], Coello-Cabezas Julio[5].

[1]Grupo de Investigación en Materiales Avanzados (GIMA), Escuela Superior Politécnica de Chimborazo (ESPOCH), Riobamba, Chimborazo 060106, Ecuador
[2]Investigadora Independiente, Riobamba, Chimborazo 060106, Ecuador
[3]Grupo de Investigación y Desarrollo en Agroindustria (IDEA), Escuela Superior Politécnica de Chimborazo (ESPOCH), Riobamba, Chimborazo 060106, Ecuador
[4]Escuela Superior Politécnica del Chimborazo (ESPOCH), Facultad de Ciencias, Riobamba, Chimborazo 060106, Ecuador
[5]Grupo de Investigación en Materiales Avanzados (GIMA), Escuela Superior Politécnica de Chimborazo (ESPOCH) – Sede Orellana, Francisco de Orellana, Orellana 220150, Ecuador.

Corresponding author.
E-mail addresses: rormaza@espoch.edu.ec (Ormaza R.).

ORCID:

Ormaza Rosa, **orcid:** 0000-0002-1917-5084
Mayorga Yajaira, **orcid:** 0000-0002-6519-9386
Mejía Nora, **orcid:** https:0000-0002-0308-5412
Aguilar Reyes Johanna: 0000-0002-1230-2503
Coello-Cabezas Julio, **orcid:** 0000-0002-4823-6763

1. Abstract

In this investigation, polymeric hydrogels with inclusions of magnetic nanoparticles (NPMs) were synthesized by reverse microemulsion polymerization method. Two stages were considered; the synthesis of the NPMs and the structuring of the hydrogel functionalized with the NPMs. A factorial design was used with 27 treatments with two replicates each, analyzing the influence of three factors: polymer concentration, melting temperature and homogenization time on the degree of saturation of the resulting hydrogels. Concentrations of 0.04, 0.05 and 0.06% by mass of agarose, combined at 50, 60 and 70°C for intervals of 7, 10 and 15 minutes were considered for homogenization. The samples were characterized by IR spectroscopy, scanning electron microscopy and refractometry; the presence of functional groups such as hydroxyl with a peak at 3311.18cm^{-1}, at 709cm^{-1} the Fe-O-Fe bond of hematite and the characteristic peak of agarose at 994.125cm^{-1}, attributed to the 3,6 anhydrous galactose bond. In addition, the homogeneous distribution presented by the NPMs around the hydrogel could be observed. The best results were obtained when applying the medium level of treatment (0.05% agarose), providing an average Brix percentage of 69.59%. It is concluded that the hydrogel synthesized is chemically stable, with a homogeneous distribution of NPMs in its structure, which do not saturate the sample, allowing the possibility of its subsequent use in the carriage of substances.

Keywords:
Polymeric hydrogel, magnetic nanoparticle, inverse microemulsion, magnetite, agarose

2. Introduction

The nanotechnology field began its development with ultrafine particles, worldwide at the end of the 1980s. Currently, the United States, Germany and China are the leading countries in the developing world that are also researching and beginning to produce nanotechnology. The major Northern power in the year 2000 generated the National Nanotechnology Initiative, obtaining promising results in Latin America, mainly in countries such as Brazil and Argentina, but also in small countries such as Uruguay, Peru, or Chile; and, even in small numbers, there is also research in Guatemala, El Salvador, and Ecuador [1], [2]

Specifically speaking of nanomaterials (NMs), it is known that they are used in several fields of science, industry, and health, all in research and teaching activities, including biomedical areas [3]. These applications require that the particles utilized are stable and can be applied, for example, in coatings and nanocomposites to improve their bioactivity and in the early detection of diseases [4], [5].

An interesting type of NMs is magnetic nanoparticles (MNPs), which have made considerable progress in recent years, mainly due to their role in the development of new materials and the great prospects for their use in biomedical and biotechnological sciences. These materials have interesting advantages such as their low cost, size, ease of manipulation by an external magnetic field gradient and, in general, their ability to be modified to unify biological agents[6].

On the other hand, hydrogels are a type of material that possess polymeric characteristics: they are hydrophilic, soft and elastic in the presence of water they considerably increase their volume (collapse or expansion), keeping their shape until they reach the necessary physical-chemical balance, which is why some hydrogels are considered intelligent materials [7], [8]. Due to the polymeric nature of these elements and their capacity to absorb large amounts of water, they can be synthesized by altering certain parameters that cause changes in their structure and composition according to the initial requirements; making possible the addition of certain materials such as NPMs in their structure, to give them new properties [9], [10].

The use of hydrogels is part of everyday life, its origins date back to the late fifties, when scientists Wichterle and Lim reported the preparation of a 2-hydroxyethyl methacrylate gel (HEMA), which was used as a material for flexible contact lenses; its biocompatibility was tested during its clinical use in implants[11]. Likewise, they are used as absorbents for diapers and feminine pads, for separating in analytical chemistry, for the preparation of elastics, for the controlled release of drugs and the design and construction of numerous biomedical applications [1], [12], [13].

Based on the mentioned above, in the following research, a hydrogel was synthesized with polymeric envelope characteristics with high stability, high anti-adherent capacity and biocompatibility, and which preserves its properties by including the NPMs. Within this study, the physicochemical properties of the hydrogel were also analyzed, such as the morphology and distribution of the NPMs within the hydrogel [9].

3. Materials and Methods

3.1. *Synthesis and purification of magnetic nanoparticles (NPMs)*

The synthesis of NPMs was carried out following the technique established in the study *"Synthesis and characterization of magnetic iron (magnetite) nanoparticles*"[14], where the co-precipitation method under the surface adsorption modality is outlined.

3.2. *Synthesis of polymeric hydrogels with NPM inclusions*

The method applied in this process is a compilation of techniques described in studies such as "*Thermosensitive nanostructured hydrogels synthesized by reverse microemulsion polymerization*" [15], "*Design, synthesis and physicochemical characterization of a nano functionalized hydrogel based on polyethylene glycol*" [16] and "*Size control of polymeric magnetic microfibers during the synthesis process"*[17]; which were adapted to the needs and material availability of the case.

First, a system of equipment and materials was built, the vibra cell sonicator was placed on the magnetic stirrer-heater with the help of two universal supports; then a crystallization beaker with distilled water was placed on top of the stirrer so that it was placed under and in the center of the sonicator (see figure 1). With the help of a clamp a beaker was installed inside (this will make the bain-marie effect), and the beakers involved needed to be kept firmly in their position.

Figure 1. System for hydrogel synthesis.

A solution of 50 mL of edible oil, 10 mL of surfactant (glycerin) and 1.5 mL of crosslinker (shampoo) was prepared. It is relevant to mention that glycerin was used as surfactant since its value according to Griffin's scale is 3.8 HBL (Hydrophilic-lipophilic balance), which defines it as a lipophilic W/O emulsifier [18]; and the shampoo as cross-linking agent because it contains sodium lauryl sulfate in its composition, and leads to the formation of the cross-linked structure of the gel [19]. This dissolution will later be called dissolution 1.

Proceeding with the process, 10 mL of solution 1 was weighed into a 50 mL beaker. In a 25 mL beaker, 1 g of NPMs was weighed, considering the different mass concentrations of agarose, this mixture was named solution 2. The beaker containing solution 1 was placed inside the water bath (at the required temperature for each treatment) and the sonicator was turned on with a wave amplitude of 50. Finish this time, the beaker was removed from the bain-marie and the gel obtained was placed in a petri dish.

4. Characterization of the polymeric hydrogel with NPMs inclusions.

4.1. *IR absorption spectrophotometry*

To identify the characteristic functional groups of the samples, the JASCO FT/IR-4100 IR spectroscope and Spectra Manager software were used. After cleaning the sample area with alcohol and absorbent cotton, a background check was performed to ensure that there were no external substances that could interfere with the analysis[20].

4.2. *Refractometry*

To obtain quantitative results to establish the influence of the variation of the agarose concentration, melting temperature, and homogenization time in the hydrogel synthesis, a refractometry analysis was performed. Kyoto Kem Electronics equipment was used, model: RA - 620 with refractive index: ±0.00002 nD[21], [22].

4.3. *Scanning electron microscopy*

To determine the details of the gel morphology, a JEOL model JSM-IT100LA Scanning Electron Microscope (SEM/EDS) was used. The three best samples were chosen, and these were cut into thin gel sheets, which were placed on a carbon tape whose function is to increase the conductivity of these for better analysis in the equipment. Voltages between 5 and 15 KeV were established; and the structures of interest were focused at x30, x800 and x1000 magnifications. Likewise, EDS analysis was performed, which provides a percentage elemental composition spectrum of the selected sample area.

5. Results and Discussion

5.1. *Results in IR spectrophotometry*

Graph 1, shows a comparison between the IR spectrums of a) the NPMs, b) the polymeric hydrogel with NPMs. The spectrum is displayed in a graph of transmittance (a.u) vs wavenumber (cm^{-1}), obtained on a scale from 580 to 4180 cm^{-1}; in this way, the composition of the samples can be identified. Graph 1-a shows the spectrum of the NPMs prior to hydrogel synthesis. While graph 1-b shows the spectrum obtained from the functionalized polymeric hydrogel belonging to the T14 treatment. In the last one, the functional groups present were identified; characteristic absorption bands for specific links or elements within the synthesized hydrogels, which were found in the bibliography [23].
A greater number of peaks is observed in the second spectrum due to the number of chemical substances in its composition, which absorb the light incident on the sample.

a) Spectrum of NPMs

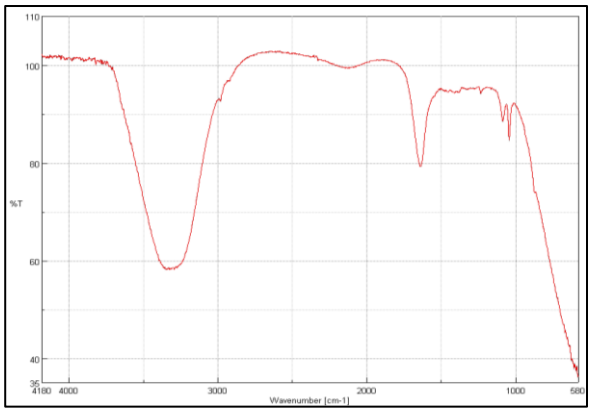

b) Spectra of polymer hydrogel with NPMs

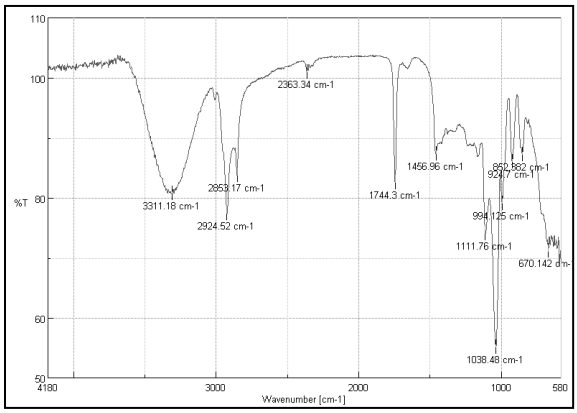

Graph 1. IR spectrums of the samples

Graph 1 shows absorption bands at 3311.18 cm^{-1} corresponding to OH bonds of the hydroxyl functional group The ranges at 2924.52, 2853.17 and 2363.34 cm^{-1} are generally observed for covalent interactions corresponding to C-H bonds [23]. Between 1749.3 and 1456.96 cm^{-1}, we find ranges that can be associated with vibrations related to the element oxygen (O), i.e., C=O and C-O-C bonds; which is representative of agarose [8], [24]–[26]. The literature also tells us that the range at 670,142 cm^{-1} cans be attributed to the presence of iron oxide NPs. Likewise, the presence of NPMs was confirmed by the peaks between 852.382 and 670.142 cm^{-1}, which may be due to the vibration produced by the stretching of the hematite core, corresponding to the Fe-O-Fe bond, specifically at 709 cm^{-1} [27]. Finally, one of the most representative peaks is at 994.125 cm^{-1}, corresponding to the presence of the 3,6 anhydrogalactose bond, component and main characteristic of agarose [24], [28].

5.2. Scanning Electron Microscopy Results

5.2.1. Polymeric hydrogels

Hydrogels with inclusions of NPMs were developed, using NPMs of sizes between 10 and 30 nm, whose average is around 15 nm, with irregular morphology characteristic of these materials.
For this analysis, the four best samples of the hydrogels were chosen, based on the results previously obtained by IR spectrophotometry and refractometry.

Figure 2 shows one of the images obtained in the SEM of the polymeric hydrogel functionalized with the NPMs, performed at 15 kV and 100 µm. This image corresponds to the medium-level treatment for the synthesis of the hydrogel with a mass concentration of 0.05% agarose, at 50°C and for 10 min.

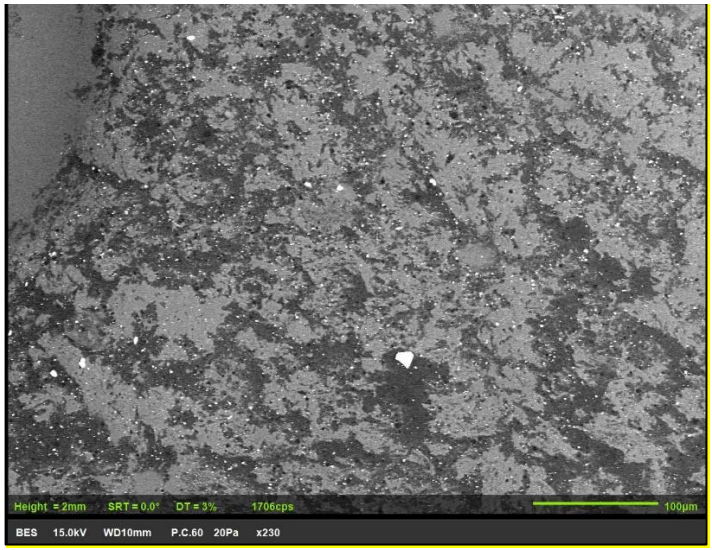

Figure 2. Polymeric hydrogel functionalized with NPMs in SEM at 15 kV.

Homogeneous distribution of the NPMs within the polymeric hydrogel can be said to exist, which is attributed to their interaction with the polymer (agarose); these results are like those found in the literature [28], [29].

Employing EDS analysis, it was possible to verify elements that corroborate the chemical nature of the hydrogel expressed in its IR spectrum; we have iron (Fe), carbon (C) and oxygen (O) as the main ones. The details of this analysis are shown in Figure 3, where it is also evident the voltage at which the image was acquired and the concentration of the elements that compose the sample.

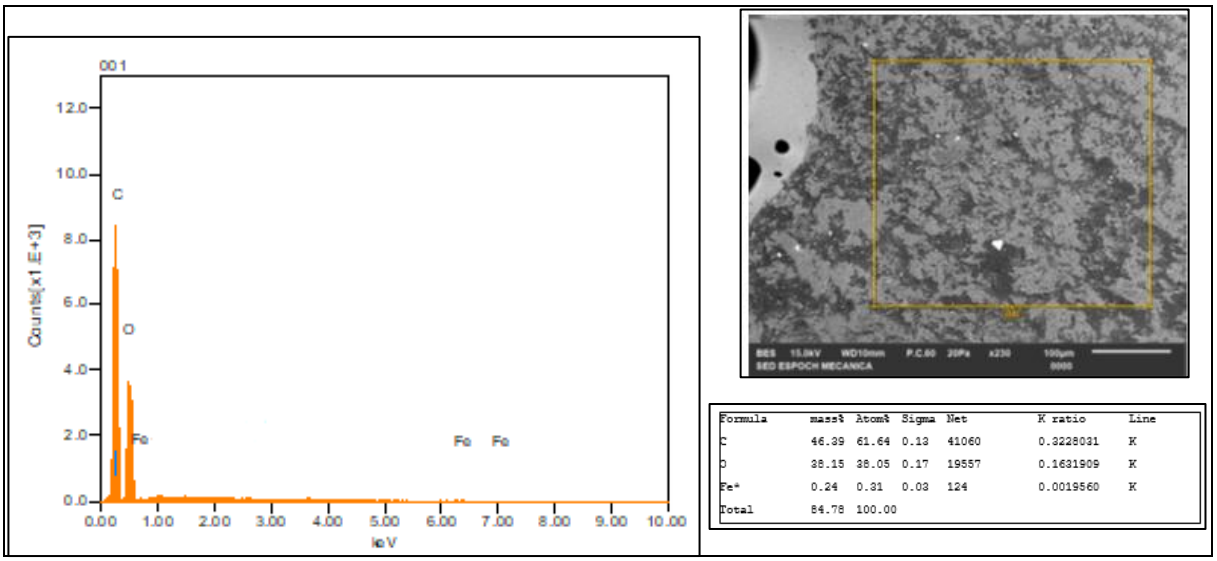

Figure 3. EDS / SEM spectra report of hydrogel

5.3. *Refractometric Results*

Based on the refractometry analysis, it was possible to develop statistical analyses that evidenced important points of this research (Table 1). We aimed to determine the influence of the variation of the agarose concentration, melting temperature and homogenization time in the synthesis of the

hydrogel. Specifically, for refractometry, the concentration of NPMs within the hydrogel, determined by the percentage of Brix degrees of the hydrogel, was the experimental unit [30].

Table 1. Experimental results of Brix measurement for each hydrogel treatment.

Treatment level	Treatment	Brix degrees (%)		Treatment	Brix degrees (%)	
Low	**T1**	65,48	63,85	**T6**	62,62	65,33
	T2	69,44	73,92	**T7**	72,84	72,84
	T3	62,50	61,16	**T8**	71,66	73,28
	T4	69,85	73,50	**T9**	73,49	73,13
	T5	65,73	65,88			
Medium	**T10**	63,34	63,31	**T15**	70,26	73,75
	T11	64,71	63,07	**T16**	63,62	69,34
	T12	71,98	68,42	**T17**	71,96	72,07
	T13	69,30	70,24	**T18**	73,20	72,49
	T14	70,41	73,46			
High	**T19**	68,63	68,59	**T24**	70,51	72,52
	T20	73,46	73,46	**T25**	70,19	68,36
	T21	73,71	72,19	**T26**	68,51	71,44
	T22	73,48	71,89	**T27**	74,00	73,68
	T23	74,11	71,54			

5.4. Statistical analysis

5.4.1.ANOVA model assumptions.

Based on the data presented in Table 1, the assumptions were made using Excel spreadsheets. Some of the values obtained in the study are proposed, just to understand the parameters considered (Table 2).

Table 2. Predicted values and residuals for the Brix percentages of hydrogel.

Observed value	Predicted value	Error	Ordered error	i	α=(i-0,5)/36	Zα
65,48	65,85	-0,37	-7,26	1	0,02	-2,11
63,85	65,85	-2,00	-6,38	2	0,04	-1,80
69,44	66,38	3,06	-6,11	3	0,05	-1,60
73,92	66,38	7,54	-4,88	4	0,07	-1,45
62,50	67,27	-4,77	-4,77	5	0,09	-1,33
74,11	71,25	2,86	3,14	45	0,83	0,96
71,44	72,97	-1,53	3,94	52	0,96	1,77
74,00	73,86	0,14	5,92	53	0,98	2,07
73,68	73,86	-0,18	7,54	54	1,00	3,11

Based on the data obtained, some of which were expressed in Table 3, graphs of normality, constant variance and independence were made to corroborate each of the assumptions.

5.4.2.Normality assumption.

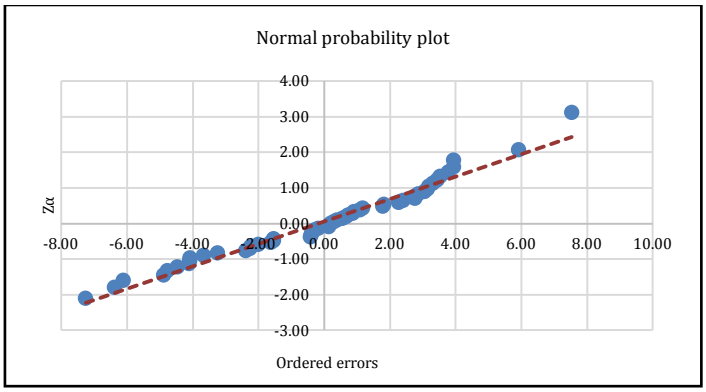

Graph 2. Normality test

In graph 2, the residuals show an increasing trend, where only one of them is towards an extreme (7.54). By drawing a straight line, most of these results are on the line or close to it. This means that the points are acceptably aligned on a straight line, which indicates that the normal distribution of the residuals suggests that the assumption of normality in the errors is fulfilled.

5.4.3. Constant variance and independence assumption

Figure 3 provides evidence of constant variance and independence assumptions. For the verification of the constant variance assumption, the predicted values and the residuals were plotted. According to graph 3-a, it can be observed that the points appear to be randomly spread; moreover, they do not follow any pattern along a horizontal line around zero. This suggests that the assumption of constant variance in the errors is true, meaning that there is no significant variability among the residuals, or they are close to zero. To test the independence assumption, it was necessary to plot the residual errors and the rank order. When observing graph 3-b, the points are randomly dispersed, which suggests that the independence hypothesis is fulfilled, i.e., the residuals are not related.

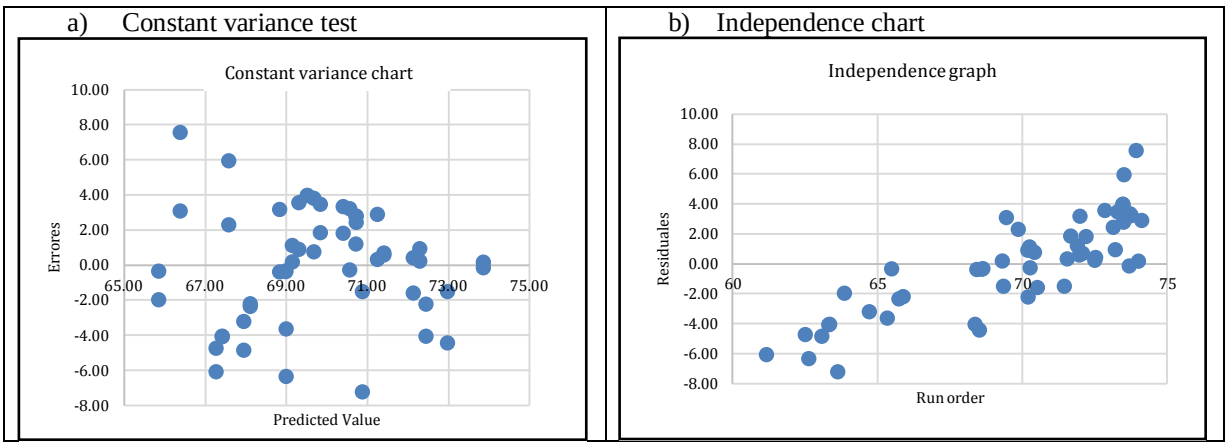

Table 3 provides the results of the ANOVA used for the three-factor design, based on the values obtained after the characterization of the 54 samples as shown.

Table 3. ANOVA of the three-factor design

F.V	S.C	GL	CM	F	Valor *p*
Factor A	99,32	2	49,66	17,47	0,000013568984
Factor B	112,91	2	56,46	19,86	0,000004970158
Factor C	34,81	2	17,41	6,12	0,006418324604
A*B	134,90	4	33,73	11,86	0,000010860070
A*C	110,61	4	27,65	9,73	0,000052581021
B*C	87,80	4	21,95	7,72	0,000277405295
A*B*C	104,88	8	13,11	4,61	0,001237116505
Residuals	76,76	27	2,84		
Total	761,99	53	14,38		

With a 95% confidence level, the non-hypothesis (H_0), is rejected and, in general, it is determined that all the main factors, as well as their interactions, are significant due to the p-value presented by each one, which is less than the 0.05 significance level. In other words, depending on the level at which each of the factors is found, they influence the Brix percentage of the hydrogel. Given that for the corresponding hypotheses to factors A, B and C expressed in Table 4-2, the p value is almost null, H_0 is rejected, and it was determined that both the polymer concentration, the melting temperature and the homogenization time significantly influence the final percentage of Brix degrees of the hydrogel.

The hypotheses of the interaction effect AB, AC and BC, since the p-value is almost null at a significance level of 5%, H_0 is rejected, and it was determined that the interaction of these factors influences the Brix percentage of the hydrogel.

Likewise, for the hypothesis of the ABC factor, because p also showed an almost null value with a significance level of 5%, H_0 is rejected, and as a result it is shown that the interactions between polymer concentration, melting temperature and homogenization time influence the percentage of Brix degrees of the hydrogel.

The most effective treatment for hydrogel synthesis was identified using the regression model associated with the fixed effects model. Since the aim is to analyze the distribution of the NPMs within the hydrogel, the Brix percentage was used as an indicator of its saturation, thus looking for the lowest percentage to maintain an equilibrium. With this study it was possible to observe that for medium concentrations the lowest values in Brix percentages were obtained for both observed values and the values predicted by the systems.

As a result of the analysis, it can be proposed that the polymer concentration of 0.05% by mass would be the most appropriate, since at a melting temperature of 50°C, 60°C or 70°C and homogenization time of 7, 10 or 15 minutes, it is presented as a winning treatment. In other words, the results using the medium level concentration are beneficial for all its combinations.

6. Conclusions.

This study was able to synthesize a polymeric hydrogel using inverse microemulsion polymerization, finding that this method allows obtaining a more stable emulsion, which maintains the NPMs on its inside, although it requires the use of a large amount of surfactant. Consequently, the chemically cross-linked hydrogel is considered to have non-sensitive stimulus characteristics. It was evidenced that by varying the temperature and homogenization time in the synthesis of the samples, crosslinking occurred, creating chemical (covalent) or physical (hydrogen bridges and van der Waals forces) bonds in the chains of the polymeric network, which gave the characteristic stability of the hydrogel, thus determining that the ideal treatment for hydrogels is at 0.05% mass concentration of the polymer.

The refractometry results showed values with an average of 69.59% Brix degrees, establishing that the amount of NPMs is high, however, it does not saturate the sample, opening the possibility of its

later use in the transport of substances. Finally, it was statistically possible to determine that the best treatment for the synthesis of hydrogels is obtained by using a 0.05% agarose concentration, without factors such as time and temperature having a significant influence on it.

7. References

[1] G. Foladori and N. Invernizzi, "Implicaciones sociales y ambientales del desarrollo de las nanotecnologías en América Latina y el Caribe," *México*, p. 40, 2012.

[2] I. A. Flores-Urquizo, P. García-Casillas, and C. Chapa-González, "Desarrollo de nanopartículas magnéticas Fe+32 X+21 O4 (X= Fe, Co y Ni) recubiertas con amino silano," *Rev. Mex. Ing. biomédica*, vol. 38, no. 1, pp. 402–411, Jan. 2017, doi: 10.17488/RMIB.38.1.36.

[3] A. K. Gaharwar, N. A. Peppas, and A. Khademhosseini, "Nanocomposite hydrogels for biomedical applications," *Biotechnol. Bioeng.*, vol. 111, no. 3, pp. 441–453, Mar. 2014, doi: 10.1002/BIT.25160.

[4] J. Ma. A. Maestro and J. I. Ma. Carbajo, "Aplicaciones Industriales de la Nanotecnología," *Proy. Nano-SME*, p. 92, 2012, [Online]. Available: https://www.idepa.es/documents/20147/163848/AplicacionesIndustriales.pdf/6c110c65-76ef-fdfb-15dd-38c072d6e2ee

[5] P. Schexnailder and G. Schmidt, "Nanocomposite polymer hydrogels," *Colloid Polym. Sci.*, vol. 287, no. 1, pp. 1–11, Oct. 2009, doi: 10.1007/S00396-008-1949-0/METRICS.

[6] M. P. Pacheco, M. G. Aquino, and E. T. Calanchi, "Síntesis y caracterización de nanopartículas superparamagnéticas obtenidas por precipitación en microemulsión inversa para aplicaciones biomédicas," *Rev. la Soc. Química del Perú*, vol. 79, no. 2, pp. 99–106, 2013.

[7] I. Katime, "Hidrogeles inteligentes," *Rev. Iberoam. Polímeros*, vol. 5, no. 5, p. 10, 2000, [Online]. Available: http://www.reviberpol.iibcaudo.com.ve/pdf/publicados/katime.pdf%0Ahttp://www.ehu.es/reviberpol/pdf/AGO06/gascue.pdf

[8] I. A. Katime Amashta, D. Katime Trabanca, and O. Katime Trabanca, "Los materiales inteligentes de este milenio los hidrogeles macromoleculares : síntesis, propiedades y aplicaciones," *An. la Real Soc. Española Química*, p. 335, 2004.

[9] A. Ramirez, J. L. Benítez, L. R. De Astudillo, and B. R. De Gáscue, "Materiales polimeros de tipo hidrogeles: Revisión sobre su caracterización mediante FTIR, DSC, MEB y MET," *Rev. Latinoam. Metal. y Mater.*, vol. 36, no. 2, pp. 108–130, 2016.

[10] S. Bashir *et al.*, "Fundamental Concepts of Hydrogels: Synthesis, Properties, and Their Applications," *Polym. 2020, Vol. 12, Page 2702*, vol. 12, no. 11, p. 2702, Nov. 2020, doi: 10.3390/POLYM12112702.

[11] M. Biondi, A. Borzacchiello, L. Mayol, and L. Ambrosio, "Nanoparticle-Integrated Hydrogels as Multifunctional Composite Materials for Biomedical Applications," *Gels 2015, Vol. 1, Pages 162-178*, vol. 1, no. 2, pp. 162–178, Oct. 2015, doi: 10.3390/GELS1020162.

[12] E. Rogel-Hernández, A. Licea-Claveríe, J. M. Cornejo-Bravo, and K.-F. Arndt, "Preparación

de hidrogeles anfifílicos sensibles a diferentes valores de pH utilizando monómeros ácidos con espaciadores hidrofóbicos," *Rev. la Soc. Química México*, vol. 47, no. 3, pp. 251–257, 2003.

[13] A. Mora, D. Jumbo-Flores, M. González-Merizalde, and S. A. Bermeo-Flores, "Niveles de metales pesados en sedimentos de la cuenca del río puyango, Ecuador," *Rev. Int. Contam. Ambient.*, vol. 32, no. 4, pp. 385–397, 2016, doi: 10.20937/RICA.2016.32.04.02.

[14] F. S. Vera Moreno, R. M. Ormaza Hugo, J. R. Coello Cabezas, V. N. Yanchapanta Bastidas, and S. E. Gusqui Macas, "APLICACIÓN DE UN DISEÑO EXPERIMENTAL COMPLETAMENTE AL AZAR PARA DETERMINAR LA VARIABILIDAD DE TAMAÑOS EN LA SÍNTESIS DE NANOPARTÍCULAS MAGNÉTICAS DE HIERRO.," *Cienc. Digit.*, vol. 2, no. 4.1., 2018, doi: 10.33262/cienciadigital.v2i4.1..195.

[15] J. A. Cortés, J. E. Puig, J. A. Morales, and E. Mendizába, "Thermosensitive nanostructured hydrogels synthesized by inverse microemulsion polymerization," *Rev. Mex. Ing. Quim.*, vol. 10, no. 3, pp. 513–520, 2011.

[16] X. González Velázquez, "Diseño, síntesis y caracterización fisicoquímica de un hidrogel nanofuncionalizado basado en polietilenglicol," Jun. 2016, Accessed: Feb. 17, 2023. [Online]. Available: http://ri.uaemex.mx/handle/20.500.11799/65404

[17] R. M. Ormaza Hugo, J. R. Coello Cabezas, and E. F. Basantes Basantes, "Control del tamaño de microfibras magnéticas poliméricas durante el proceso de síntesis.," *Cienc. Digit.*, vol. 3, no. 1, pp. 176–186, 2019, doi: 10.33262/cienciadigital.v3i1.273.

[18] A. Gadhave, "Determination of Hydrophilic-Lipophilic Balance Value," vol. 3, no. 4, pp. 573–575, 2014.

[19] C. Chacón Vera, N. Pérez, and M. Sabino G., "Efecto de la cantidad de fase interpenetrada lignocelulósica y la composición sobre el proceso de hinchamiento y síntesis de hidrogeles interpenetrados en base a acrilamida," *Rev. Iberoam. Polímeros*, vol. 17, no. 4, pp. 170–182, 2016.

[20] M. N. Toala Paola, Coello-Cabezas Julio, Ormaza Rosa, "INACTIVATION OF PHOSPHORUS IN EUTROPHIC WATERS THROUGH THE APPLICATION OF MAGNETITE NANOPARTICLES," *An Interdiscip. J. Neurosci. Quantum Phys.*, vol. Volume 20, no. No 7, pp. 908–916, 2022, doi: 10.14704/NQ.2022.20.7.NQ33115.

[21] H. Isakau, M. Robert, and K. I. Shingel, "A novel derivatization-free method of formaldehyde and propylene glycol determination in hydrogels by liquid chromatography with refractometric detection," *J. Pharm. Biomed. Anal.*, vol. 49, no. 3, pp. 594–600, Apr. 2009, doi: 10.1016/J.JPBA.2008.10.038.

[22] A. P. Titrator, K. Fischer, M. Titrator, G. V. Analyzer, A. Meter, and T. M. Instrument, "Refractometer".

[23] H. F. Shurvell, "Spectra- Structure Correlations in the Mid- and Far-Infrared," in *Handbook of Vibrational Spectroscopy*, 2006. doi: 10.1002/0470027320.s4101.

[24] Z. Xu, R. Zhao, X. Huang, X. Wang, and S. Tang, "Fabrication and biocompatibility of agarose acetate nanofibrous membrane by electrospinning," *Carbohydr. Polym.*, vol. 197, no. June, pp. 237–245, 2018, doi: 10.1016/j.carbpol.2018.06.004.

[25] A. Awadhiya, D. Kumar, and V. Verma, "Crosslinking of agarose bioplastic using citric acid," *Carbohydr. Polym.*, vol. 151, pp. 60–67, 2016, doi: 10.1016/j.carbpol.2016.05.040.

[26] J. L. Escobar, D. M. García, D. Zaldivar, and I. Katime, "Hidrogeles. Principales Características en el diseño de sistemas de liberación controlada de fármacos.," *Rev. Iberoam. Polímeros*, vol. 3, no. 3, pp. 1–28, 2002.

[27] L. Li, D. Qin, X. Yang, and G. Liu, "Synthesis of ellipsoidal hematite/polymer/titania hybrid materials and the corresponding hollow ellipsoidal particles," *Polym. Chem.*, vol. 1, no. 3, pp. 289–295, 2010, doi: 10.1039/b9py00230h.

[28] R. M. Ormaza Hugo, J. R. Coello Cabezas, and E. F. Basantes Basantes, "Control del tamaño de microfibras magnéticas poliméricas durante el proceso de síntesis.," *Cienc. Digit.*, vol. 3, no. 1, 2019, doi: 10.33262/cienciadigital.v3i1.273.

[29] U. S. K. Madduma-Bandarage and S. V. Madihally, "Synthetic hydrogels: Synthesis, novel trends, and applications," *J. Appl. Polym. Sci.*, vol. 138, no. 19, p. 50376, May 2021, doi: 10.1002/APP.50376.

[30] J. M. González-Méijome, M. Lira, A. López-Alemany, J. B. Almeida, M. A. Parafita, and M. F. Refojo, "Refractive index and equilibrium water content of conventional and silicone hydrogel contact lenses," *Ophthalmic Physiol. Opt.*, vol. 26, no. 1, pp. 57–64, Jan. 2006, doi: 10.1111/J.1475-1313.2005.00342.X.